Real Time Single Image Dehazing and Soil Removal Using CNNs

Wajahat Akhtar
Adasens Automotive GmbH
Lindau (Bodensee), Germany
wa19@hw.ac.uk

Sergio Roa-Ovalle
Adasens Automotive GmbH
Lindau (Bodensee), Germany
sergio.roa-ovalle@ficosa.com

Florian Baumann
Adasens Automotive GmbH
Lindau (Bodensee), Germany
florian.baumann@ficosa.com

ABSTRACT

Removal of atmospheric haze and soil from a single image captured via monocular camera is very challenging and computationally ill-posed phenomenon in the advanced driver assistance systems (ADAS). The recent development in the field of deep learning has made it possible for the researchers to train a model using various available on-the-shelf tools. However, such models are not adapted to embedded platforms due to their deep architecture design. In this paper, we propose a new Convolutional Neural Network (CNN) based architecture design, which inspires from EVD-Net j-level fusion and AOD-Net for real-time single image dehazing and soil removal for an embedded platform. The CNN is designed based on a reformulated atmospheric scattering model for haze and soil removal called Haze and Soil Removal Using Convolutional Neural Network (HSRCNN). This is a first fully end-to-end CNN model for real-time single image *dehazing* and *soil removal*. The model is trained and tested using our own generated dataset for both haze and soil. Furthermore, a pre-trained faster R-CNN is used to verify the performance difference between haze and soil images as compared to clean images. Lastly, we witnessed a great improvement especially, in image quality and object detection. HSRCNN is applicable to a variety of distinct scenarios like ADAS, medical imaging, night imaging and underwater imaging. The lightweight design makes it easier to cascade with other neural networks. The model is also tested and evaluated using different public datasets such as RESIDE.

CCS CONCEPTS

• **Computing methodologies** → **Artificial intelligence**; Computer Vision; Image and video acquisition; Computer vision tasks; Computer vision problems; Object detection; Object recognition; Machine learning; Learning paradigms; Supervised learning; • **Computer systems organization** → *Architectures*;

ACM ISBN 978-1-4503-6616-8/18/09...$15.00
https://doi.org/10.1145/3273946.3273954

KEYWORDS

Deep learning, convolutional neural networks, haze removal, soil removal, image dehazing, noise removal, advanced driver assistannce systems, poor weather conditions

ACM Reference Format:
Wajahat Akhtar, Sergio Roa-Ovalle, and Florian Baumann. 2018. Real Time Single Image Dehazing and Soil Removal Using CNNs. In *2nd Computer Science in Cars Symposium - Future Challenges in Artificial Intelligence & Security for Autonomous Vehicles (CSCS 2018), September 13–14, 2018, Munich, Germany*. ACM, New York, NY, USA, 6 pages. https://doi.org/10.1145/3273946.3273954

1 INTRODUCTION

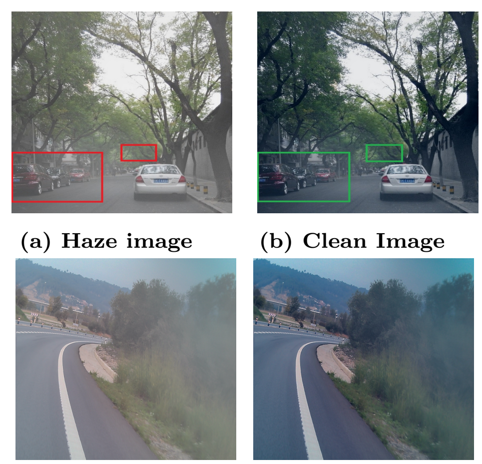

(a) Haze image **(b) Clean Image**

(c) Soil Image **(d) Clean Image**

Figure 1: Visual quality results of HSRCNN on haze and soil covered images using (Top row) RESIDE [15], and (Bottom row) our automotive dataset.

Advanced Driver Assistance Systems (ADAS) is a rising upcoming technology to improve road safety, autonomous driving, driver comfort and to reduce energy consumptions[1]. ADAS use a monocular camera for autonomous parking, object detection, lane change recognition and surround view system to ensure reliability. However, the detection and recognition qualities are strongly affected by frequent haze such as aerosols in the atmosphere as discussed by Hwang and Lee*

[1] http://telematicswire.net/bmw-driving-into-the-automotive-future-with-adas/

in [10], and soil on camera lens e.g dust, sand, silt and clay, Gu et al. in Gu et al. [6]. Therefore, haze and soil removal has become a notable trouble in ADAS for autonomous vehicles. The presence of haze due to poor weather conditions can hinder the images that are being acquired by the camera causing poor quality image acquisition and poor visibility as shown in Figure 1. The light scattered by haze and soil can deteriorate not only the aesthetic beauty of the scene but also occludes important salient features in the image. Hence, significantly reduces the performance of an algorithm. Most recently, with an advancement in deep learning, people have proposed different methods for haze and soil removal. Computer vision has become an attractive field of research in ADAS, achieving the state-of-the-art results. A common issue that exists in these methods is the computational cost, which is unsuitable for real-time implementation in ADAS. In this article, we propose a method to perform not only real-time single image haze removal using CNN but also soil removal for embedded platforms. A CNN based model has been designed for both haze and soil removal using two different mathematical formulations.

2 LITERATURE REVIEW

Haze is traditionally an atmospheric phenomenon in which images capture under bad conditions such as dust, smoke, and other dry particulates obscure the clarity of the sky [2]. Where soil is a black or dark brown material typically consisting of a mixture of organic remains, clay, and rock particles [3]. It generally appears on the cameras installed in ADAS and surveillance outdoor vision systems (SOVs).

The first mathematical model for the formation of haze was formulated by Koschmieder [12] in 1924 (see Equation 1) and was later reformulated by Li et al. [14] (see Equation 3), making it the most widely used method in the literature.

$$I(x) = J(x)t(x) + \alpha(1 - t(x)) \tag{1}$$

The model incorporates two parts: the attenuation of transmitted light $t(x)$ known as scene transmission map as in Equation (1) and $J(x)$ is the actual scene irradiance. $I(x)$ is the observed hazy image, α is the ambient formed by the scattering of the environmental illumination linked to the quantity of light illuminating the scene. Whereas, x denotes an individual pixel location in the image.

The scene transmission $t(x)$, is a function of depth and is given by:

$$t(x) = e^{-\beta d(x)} \tag{2}$$

Here, $d(x)$ is the depth of the scene point corresponding to the pixel location x. β is the haze absorption, also known as scattering coefficient of the atmosphere to represent the ability of a unit volume of atmosphere to scatter light in all directions [21] as in Equation (2).

[2]https://en.wikipedia.org/wiki/Haze
[3]https://en.wikipedia.org/wiki/Soil

$$J(x) = K(x)I(x) - K(x) + b \tag{3}$$

The reformulated model $K(x)$ for haze formation is the integration of both α and $t(x)$ with constant bias variable b.

In order to solve the second issue of soil removal, we followed the mathematical model initially presented by Gu et al. [6], as shown in Equation 4 for dirty lens artifact.

$$I(x) = I_0(x)a(x) + cb(x) \tag{4}$$

Above here, I_0 is the clean image, $\alpha(x)$ is the attenuation map (camera dependent). $c(x)$ represents aggregate of outside illumination and is scene dependent. Whereas, $b(x)$ is the scattering map and is also camera dependent.

This model is also reformulated by Eigen et al. [3] as shown in Equation 5 :

$$I' = p\alpha D + I(1 - \alpha) \tag{5}$$

I represent the original clean image, I' as generated noisily image. α is a transparency mask and D is the additive component of the soil. p is a random perturbation vector in RGB space, and the factors $p\alpha D$ are multiplied together element-wise as discussed in [3].

Deep Convolutional Neural Networks (DCNN) have shown record-shattered performance in a variety of computer vision problems. Recently CNN's has been used for image dehazing and soil removal to produce better quality and clean images. In general, when we consider supervised methods, there is always a lack of sufficient and correctly labeled data. Also, due to the deep architectures of the models, these structures are marked as less suitable for an embedded platform. Whereas, In this article, we overcome most of the aforementioned drawbacks by designing a method to generate a single clean and better quality image with real-time implementation for an embedded platform.

2.1 Traditional Methodologies

In general, there exist three kinds of methodologies in literature for haze removal : **Multiple Images** [21, 22, 25, 26] **Single Image** [4, 7, 8, 18, 20, 23, 29, 30] and using **Deep learning** [2, 14, 16, 24, 28]. Deep Learning for solving ill-posed image dehazing is quite recent (i.e 2016) whereas, for soil removal the first work was done back in 2013 by Eigen et al. [3].

Earlier methods such [21, 25] used multiple images under different weather conditions and degree of polarization to perform haze removal. While other [9] approaches resorted to estimate atmospheric scattering model parameters with the empirical Dark Channel Prior. Tan [29] provided a method to enhance the local contrast of the images based on the study that haze free images have higher contrast to non-hazy images. Hautiere et al. [7], Ma et al. [17] presented a method to remove haze from images captured from moving vehicle camera. Recently, this problem was addressed by Cai et al., Li et al., Ling et al., Ren et al., Swami and Das using deep learning.

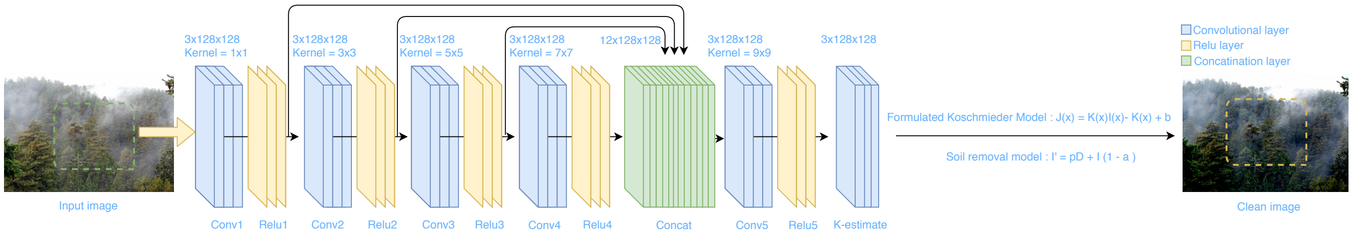

Figure 2: The proposed architecture of HSRCNN. It is constructed by 5 convolution layers, 1 concatenation layer with each layer output is passed through Relu activation function for generation of a clean haze and soil free image.

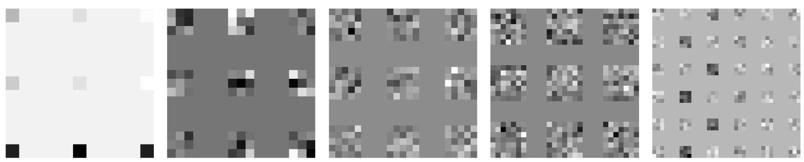

(a) Conv1 **(b) Conv2** **(c) Conv3** **(d) Conv4** **(e) Conv5**

Figure 3: Layer visualization of Proposed HSRCNN (left-right) : "conv1"-"conv5" layers and their kernels.

There exist a common problem among these methods: firstly they all are computational expensive except(AOD-Net). Secondly among all the methods in literature, very few could design models to be used for dynamic scenarios. According to the study by Ancuti et al. [1] and Silberman et al. [27] none of these methods could produce high-quality images except [28]. Due to their limitations and limited practical applicability, these methods are not being used in ADAS. We try to solve most of the above issues by presenting a novel end-to-end deep learning model to generate haze and soil free images.

2.1.1 Contribution. The main contributions in this paper are summarized as follows:

1. HSRCNN is a first real-time single image haze and soil removal CNN architecture. It directly generates clean haze and soil free image with better quality, estimating attenuation and scattering parameters jointly. Whereas, most of the methods use multiple images with significantly higher computational cost.

2. In this work, we developed a unique setup with two monocular cameras, where one camera lens is covered with soil and other is soil-free. Both cameras are adjusted and calibrated in a way that they capture the same scene. The setup is designed to acquire real images for training our soil model. It also solves the issue of labeling the dataset for soil removal. As to date there exist no single labeled public dataset online for both synthetic and real images.

3. A novel method is also established to generate synthetic dataset using real soil on cameras lens. First, different soil samples are created and images are acquired from the samples. Later, the soil is extracted from the images and used as a mask for creating synthetic datasets.

4. Most of the available dataset in the literature use homogeneous haze to generate hazy images. Whereas, we created a method to generate synthetic dataset which contains homogeneous and non-homogeneous haze for training our haze model. The images are firstly divided into patches and haze is generated using different hyper-parameter for each patch as in [14].

3 MODEL ARCHITECTURE

In this work, we formulate the constrained problem of real-time single image dehazing and soil removal for ADAS. To generate a high-quality haze and soil free image from a degraded hazy and soil carrying input image. We propose a novel end-to-end convolutional neural network (CNN) called HSRCNN. It consists of two main components: an optimized CNN network design to estimate the transmission map and a mathematical model each for haze and soil to generate a single clean image. The CNN architecture is designed based on the inspiration from the j-level fusion of EVD-Net[13] and AOD-Net [14]. To generate clean image $J(x)$, it estimates $K(x)$ from an input image $I(x)$, followed by a clean image generation module that utilizes $K(x)$ as its input-adaptive parameters to estimate clean image $J(x)$ [14] as shown in Equation 3. Whereas, for soil, we use a mathematical expression as given in Equation 5. The estimation of K is significant for our model HSRCNN as it estimates both haze and depth levels as shown in Figure 2. Our model follows solely a standard CNN model as in [2]. Each convolutional layer applies a kernel composed of $w * h * d$ coefficients, with w defining the width, h as the height and d as the depth of the hidden convolutional layers. The depth of the layers depends on the number of activation maps in the layers. Each layer is followed by an activation function to introduce non-linearity as discussed in

Table 1: Average PSNR and SSIM on Reside benchmark dataset

Metrics	DCP	MSCNN	DehazeNet	AOD-Net	HSRCNN (haze removal)
PSNR	18.87	20.01	22.26	21.01	23.231
SSIM	0.793	0.790	0.832	0.837	0.842

Table 2: Average PSNR and SSIM on our automotive soil dataset

Metrics	Dirt or Rain removal [3]	HSRCNN (soil removal)
PSNR	17.978	21.231
SSIM	0.781	0.811

(a) Haze **(b) Clean** **(c) Haze** **(d) Clean** **(e) Haze** **(f) Clean**

Figure 4: Experimental results of HSRCNN haze and soil removal on public datasets.

[19] [2]. The first layer called $conv1$ takes an input single RGB image of $size = h * w$ and d, a stride of $size = 1$ with kernel $size = 1$ results in three different activation maps, followed by layer "$relu1$" to introduce non-linearity. The second layer takes $conv1$ as its input, with stride and pad $size = 1$ and kernel $size = 3$ generating 3 activation maps, followed by a "$relu2$" layer. Similarly "$conv3$" and "$conv4$" layers were created with kernel $size = 5$, and 7. Inspired from [24], which concatenates the coarse-scale network features we create layer 5 of HSRCNN, which concatenates "$conv1$","$conv2$","$conv3$" and "$conv4$" called "$concat1$" generating three channel R-G-B output, followed by a last convolutional layer "$conv5$" of kernel $size = 9$. The output of the layer "$conv5$" i.e $'K(x)'$ is the estimated transmission map with global atmospheric light. Which is the then used as a prior in Equation 3 and Equation 5 to generate a clean image, as could be seen in Figure 2. Whereas, Figure 3 depicts the layerwise visualization of each kernel of the CNN model.

3.1 Dataset creation and Training

Training for both haze and soil model was performed separately using deep learning framework Caffe Jia et al. [11].

Haze model: As there exist no benchmark datasets for haze and its corresponding non-hazy images online except [15] which only uses homogeneous haze, we decided to create a dataset which contains both homogeneous and non homogeneous haze with different levels. The nature of haze was inspected after studying natural images as haze was non-homogeneous in nature and its concentration is not constant over the image space (the fog might be denser over a body of water due to its vaporization). A Synthetic dataset of fifty thousand training and twenty thousand validation non-overlapping hazy images were generated using our automotive and region segmented SUN2012 dataset of cleaned images. Synthetic haze was added to each segmented region[14]. The training data was converted into an hdf5 format as explained in [4]. Weights were initialized using Gaussian random variables with Relu neuron as stated in [19] and [2]. The base learning rate was set to $base_l r : 0.000001$ with $lr_p olicy$: "$step$". The model was trained with a batch-size = 100, taking five hundred iterations to complete 1 epoch. In total, the model converged in less than ten epoch (i.e five thousand total number of iterations) using Stochastic Gradient Descent "SGD".

Soil model: Similar to haze, there exist no benchmark or public datasets online for images with and without soil on a camera lens. To create a dataset with ground truth, a novel simple technique is designed to extract soil from images taken from monocular cameras. Different soil samples were created and the soil was extracted to create a labeled dataset with and without soil from real images. A dataset of thirty thousand labeled images for training and ten thousand non-overlapping soil images for testing was created as explained in section 3.1 of [3]. The training data was first converted into $hdf5$ format. Weights were initialized using Gaussian random variables with Relu neuron as for haze. The base learning rate, learning policy, step size and batch size was set accordingly. The model was trained using Tesla P100-PCIE and tested real-time on Jetson tk1.

[4] http://machinelearninguru.com/deep_learning/data_preparation/hdf5/hdf5.html

(a) Haze Image **(b) Clean Image** **(c) Haze + FastRCNN** **(d) Clean + FastRCNN**

Figure 5: Proposed HSRCNN haze removal performance evaluation using FastRCNN [5] , (left-right) : Input hazy image, generated clean image by HSRCNN, FastRCNN [5] applied on hazy input with recognition rate of 0.607, 0.964 and 0.782, FastRCNN [5] applied to generated clean image with better recognition rate such as 0.655, 0.985, 0.775. Zoom in the images to see the recognition rate clearly.

(a) Soil Image **(b) Clean Image** **(c) Soil + FastRCNN** **(d) Clean + FastRCNN**

Figure 6: Proposed HSRCNN soil removal performance evaluation using FastRCNN [5], (left-right) : Input real image captured with soil lens, generated clean image by HSRCNN, FastRCNN [5] applied on soil input with recognition rate 0.299, FastRCNN [5] applied to generated clean image with a recognition rate of 0.670. Zoom in the images to see the recognition rate clearly.

4 EXPERIMENTAL RESULTS

In this section, we compare our proposed model with several state-of-the-art methods for image dehazing and soil removal using deep learning. As stated above, we have created two different datasets each for soil and haze. To evaluate our algorithm for haze removal we use a synthesized testset RESIDE [15]. To conduct a fair test we computed PSNR and SSIM using RESIDE benchmark[15]. SSIM computes errors beyond pixel level and reflects human perception. The results we achieved as shown in Table 1 depicts that our model produces promising results both in terms of peak signal to noise ratio (PSNR) and structural similarity index (SSIM). The model HSRCNN was also evaluated using our automotive synthetic and real soil dataset as shown in Table 2. To perform some further experiments, we used public single images for soil and haze as shown in figure 1 and Figure 4. FastRCNN was used to verify the performance of HSRCNN with haze images from RESIDE as can be seen in Figure 5. Whereas, for soil removal real images from our automotive dataset was used to evaluate the performance. The experimental results show clearly that our method performs better in different scenarios removing haze and soil from the single image.

5 CONCLUSIONS AND FUTURE WORK

This article proposes a CNN model for real-time single image dehazing and soil removal for ADAS. The model was compared with state-of-the-art methods achieving results with better performance and improved image quality. A novel technique for creating synthesized and real dataset for both haze and soil was established. Moreover, our model is tested on different real and synthetic datasets to prove the robustness and efficiency under different environmental conditions. Lastly, model evaluation was performed using FastRCNN [5] to produce a clean image along with its recognition rate as compare to an un-clean image. In future, we aim to design a model called joint HSRCNN to jointly remove haze and soil from a single image with one mathematical formation.

REFERENCES

[1] C. Ancuti, C. O. Ancuti, and C. De Vleeschouwer. 2016. D-HAZY: A dataset to evaluate quantitatively dehazing algorithms. In *2016 IEEE International Conference on Image Processing (ICIP)*. 2226–2230. https://doi.org/10.1109/ICIP.2016.7532754

[2] B. Cai, X. Xu, K. Jia, C. Qing, and D. Tao. 2016. DehazeNet: An End-to-End System for Single Image Haze Removal. *IEEE Transactions on Image Processing* 25, 11 (Nov 2016), 5187–5198.

https://doi.org/10.1109/TIP.2016.2598681

[3] D. Eigen, D. Krishnan, and R. Fergus. 2013. Restoring an Image Taken through a Window Covered with Dirt or Rain. (Dec 2013), 633–640. https://doi.org/10.1109/ICCV.2013.84

[4] Raanan Fattal. 2008. Single Image Dehazing. *ACM Trans. Graph.* 27, 3, Article 72 (Aug. 2008), 9 pages. https://doi.org/10.1145/1360612.1360671

[5] Ross Girshick. 2015. Fast R-CNN. In *Proceedings of the 2015 IEEE International Conference on Computer Vision (ICCV) (ICCV '15)*. IEEE Computer Society, Washington, DC, USA, 1440–1448. https://doi.org/10.1109/ICCV.2015.169

[6] Jinwei Gu, Ravi Ramamoorthi, Peter Belhumeur, and Shree K. Nayar. 2009. Removing Image Artifacts Due to Dirty Camera Lenses and Thin Occluders. 28 (12 2009).

[7] N. Hautiere, J. P. Tarel, and D. Aubert. 2007. Towards Fog-Free In-Vehicle Vision Systems through Contrast Restoration. In *2007 IEEE Conference on Computer Vision and Pattern Recognition*. 1–8. https://doi.org/10.1109/CVPR.2007.383259

[8] K. He, J. Sun, and X. Tang. 2011. Single Image Haze Removal Using Dark Channel Prior. *IEEE Transactions on Pattern Analysis and Machine Intelligence* 33, 12 (Dec 2011), 2341–2353. https://doi.org/10.1109/TPAMI.2010.168

[9] Kaiming He, Jian Sun, and Xiaoou Tang. 2011. Single Image Haze Removal Using Dark Channel Prior. *IEEE Trans. Pattern Anal. Mach. Intell.* 33, 12 (Dec. 2011), 2341–2353. https://doi.org/10.1109/TPAMI.2010.168

[10] Seokha Hwang and Youngjoo Lee*. 2016. Sharpness-aware evaluation methodology for haze-removal processing in automotive systems. *IEIE Transactions on Smart Processing and Computing* 5, 6 (Dec. 2016), pp. 390–394.

[11] Yangqing Jia, Evan Shelhamer, Jeff Donahue, Sergey Karayev, Jonathan Long, Ross B. Girshick, Sergio Guadarrama, and Trevor Darrell. 2014. Caffe: Convolutional Architecture for Fast Feature Embedding. *CoRR* abs/1408.5093 (2014). arXiv:1408.5093 http://arxiv.org/abs/1408.5093

[12] Koschmieder. (1924). *H. Theorie der horizontalen sichtweite.* Beitr. Zur Phys. d. freien Atm 171-181.

[13] Boyi Li, Xiulian Peng, Zhangyang Wang, Jizheng Xu, and Dan Feng. 2017. End-to-End United Video Dehazing and Detection. *CoRR* abs/1709.03919 (2017). arXiv:1709.03919 http://arxiv.org/abs/1709.03919

[14] Boyi Li, Xiulian Peng, Zhangyang Wang, Ji-Zheng Xu, and Dan Feng. 2017. AOD-Net: All-in-One Dehazing Network. In *Proceedings of the IEEE International Conference on Computer Vision*.

[15] Boyi Li, Wenqi Ren, Dengpan Fu, Dacheng Tao, Dan Feng, Wenjun Zeng, and Zhangyang Wang. 2017. RESIDE: A Benchmark for Single Image Dehazing. *arXiv preprint arXiv:1712.04143* (2017).

[16] Z. Ling, G. Fan, Y. Wang, and X. Lu. 2016. Learning deep transmission network for single image dehazing. In *2016 IEEE International Conference on Image Processing (ICIP)*. 2296–2300. https://doi.org/10.1109/ICIP.2016.7532768

[17] K. Ma, W. Liu, and Z. Wang. 2015. Perceptual evaluation of single image dehazing algorithms. In *2015 IEEE International Conference on Image Processing (ICIP)*. 3600–3604. https://doi.org/10.1109/ICIP.2015.7351475

[18] G. Meng, Y. Wang, J. Duan, S. Xiang, and C. Pan. 2013. Efficient Image Dehazing with Boundary Constraint and Contextual Regularization. In *2013 IEEE International Conference on Computer Vision*. 617–624. https://doi.org/10.1109/ICCV.2013.82

[19] Vinod Nair and Geoffrey E. Hinton. 2010. Rectified Linear Units Improve Restricted Boltzmann Machines. In *Proceedings of the 27th International Conference on International Conference on Machine Learning (ICML'10)*. Omnipress, USA, 807–814. http://dl.acm.org/citation.cfm?id=3104322.3104425

[20] Srinivasa G. Narasimhan and Shree Nayar. 2003. Interactive Deweathering of an Image using Physical Models. In *IEEE IEEE Workshop on Color and Photometric Methods in Computer Vision, In Conjunction with ICCV*.

[21] S. G. & Nayar S. K Narasimhan. 2003. Contrast Restoration of Weather Degraded Images. *IEEE Trans. Pattern Anal. Mach. Intell.(TPAMI)* 25 (2003), 824–840.

[22] S. K. Nayar and S. G. Narasimhan. 1999. Vision in bad weather. In *Proceedings of the Seventh IEEE International Conference on Computer Vision*, Vol. 2. 820–827 vol.2. https://doi.org/10.1109/ICCV.1999.790306

[23] Ko Nishino, Louis Kratz, and Stephen Lombardi. 2012. Bayesian Defogging. *Int. J. Comput. Vision* 98, 3 (July 2012), 263–278. https://doi.org/10.1007/s11263-011-0508-1

[24] Wenqi Ren, Si Liu, Hua Zhang, Jinshan Pan, Xiaochun Cao, and Ming-Hsuan Yang. 2016. Single Image Dehazing via Multi-Scale Convolutional Neural Networks. In *European Conference on Computer Vision*.

[25] Y. Y. Schechner, S. G. Narasimhan, and S. K. Nayar. 2001. Instant dehazing of images using polarization. In *Proceedings of the 2001 IEEE Computer Society Conference on Computer Vision and Pattern Recognition. CVPR 2001*, Vol. 1. I–325–I–332 vol.1. https://doi.org/10.1109/CVPR.2001.990493

[26] S. Shwartz, E. Namer, and Y. Y. Schechner. 2006. Blind Haze Separation. In *2006 IEEE Computer Society Conference on Computer Vision and Pattern Recognition (CVPR'06)*, Vol. 2. 1984–1991. https://doi.org/10.1109/CVPR.2006.71

[27] Nathan Silberman, Derek Hoiem, Pushmeet Kohli, and Rob Fergus. 2012. Indoor Segmentation and Support Inference from RGBD Images. In *Proceedings of the 12th European Conference on Computer Vision - Volume Part V (ECCV'12)*. Springer-Verlag, Berlin, Heidelberg, 746–760. https://doi.org/10.1007/978-3-642-33715-4_54

[28] K. Swami and S. K. Das. 2018. CANDY: Conditional Adversarial Networks based Fully End-to-End System for Single Image Haze Removal. *ArXiv e-prints* (Jan. 2018). arXiv:cs.CV/1801.02892

[29] R. T. Tan. 2008. Visibility in bad weather from a single image. In *2008 IEEE Conference on Computer Vision and Pattern Recognition*. 1–8. https://doi.org/10.1109/CVPR.2008.4587643

[30] J. P. Tarel and N. Hautire. 2009. Fast visibility restoration from a single color or gray level image. In *2009 IEEE 12th International Conference on Computer Vision*. 2201–2208. https://doi.org/10.1109/ICCV.2009.5459251